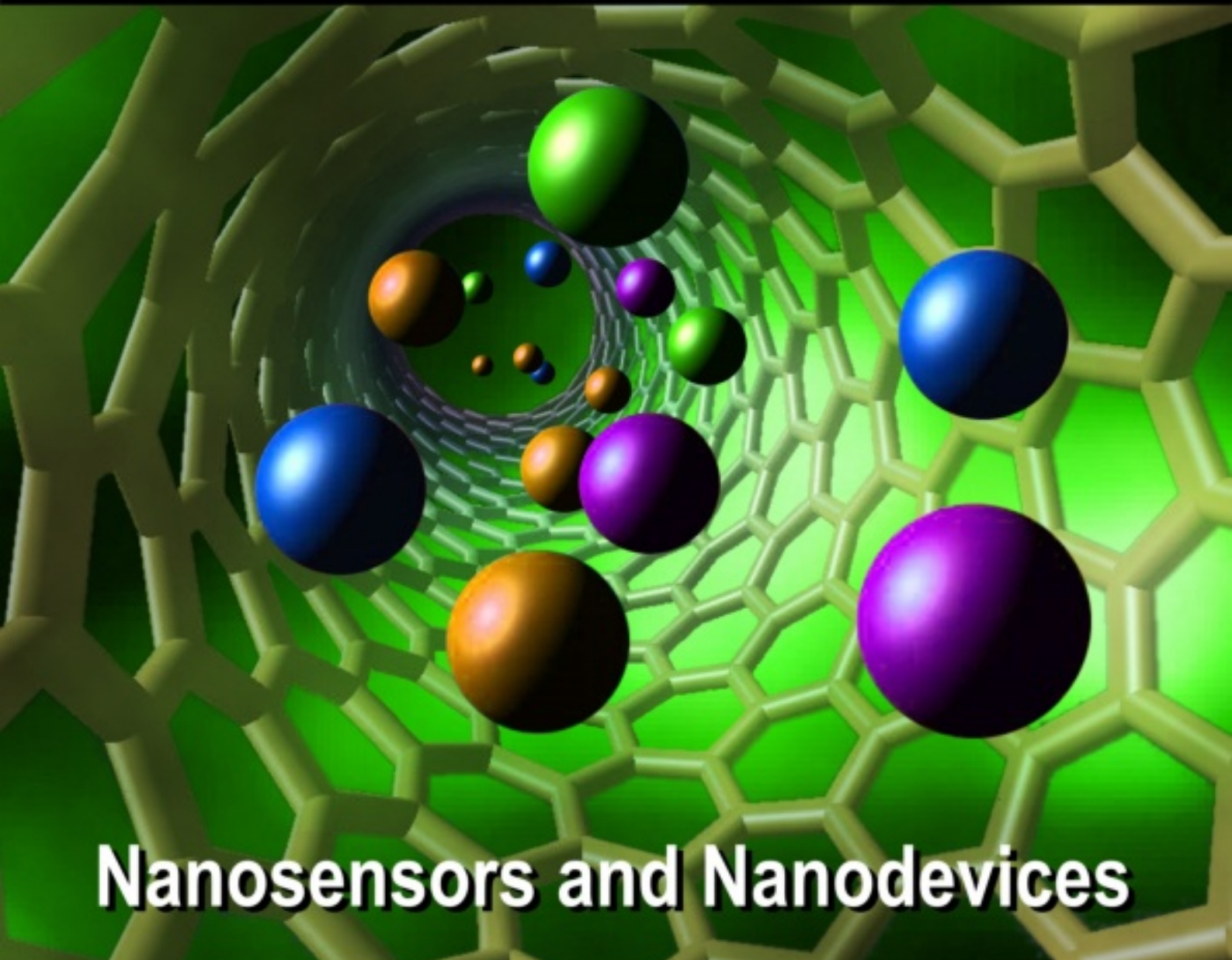


ISSN 1726-5749

SENSORS & TRANSDUCERS

11^{vol. 85}
/07



Nanosensors and Nanodevices

International Frequency Sensor Association Publishing





Sensors & Transducers

Volume 85
Issue 11
November 2007

www.sensorsportal.com

ISSN 1726-5479

Editor-in-Chief: professor Sergey Y. Yurish, phone: +34 696067716, fax: +34 93 4011989,
e-mail: editor@sensorsportal.com

Editors for Western Europe

Meijer, Gerard C.M., Delft University of Technology, The Netherlands
Ferrari, Vittorio, Università di Brescia, Italy

Editors for North America

Datskos, Panos G., Oak Ridge National Laboratory, USA
Fabien, J. Josse, Marquette University, USA
Katz, Evgeny, Clarkson University, USA

Editor South America

Costa-Felix, Rodrigo, Inmetro, Brazil

Editor for Eastern Europe

Sachenko, Anatoly, Ternopil State Economic University, Ukraine

Editor for Asia

Ohyama, Shinji, Tokyo Institute of Technology, Japan

Editorial Advisory Board

- Abdul Rahim, Ruzairi**, Universiti Teknologi, Malaysia
Ahmad, Mohd Noor, Nothern University of Engineering, Malaysia
Annamalai, Karthigeyan, National Institute of Advanced Industrial Science and Technology, Japan
Arcega, Francisco, University of Zaragoza, Spain
Arguel, Philippe, CNRS, France
Ahn, Jae-Pyoung, Korea Institute of Science and Technology, Korea
Arndt, Michael, Robert Bosch GmbH, Germany
Ascoli, Giorgio, George Mason University, USA
Atalay, Selcuk, Inonu University, Turkey
Atghiaee, Ahmad, University of Tehran, Iran
Augutis, Vygantas, Kaunas University of Technology, Lithuania
Avachit, Patil Lalchand, North Maharashtra University, India
Ayesh, Aladdin, De Montfort University, UK
Bahreyni, Behraad, University of Manitoba, Canada
Baoxian, Ye, Zhengzhou University, China
Barford, Lee, Agilent Laboratories, USA
Barlingay, Ravindra, Priyadarshini College of Engineering and Architecture, India
Basu, Sukumar, Jadavpur University, India
Beck, Stephen, University of Sheffield, UK
Ben Bouzid, Sihem, Institut National de Recherche Scientifique, Tunisia
Binnie, T. David, Napier University, UK
Bischoff, Gerlinde, Inst. Analytical Chemistry, Germany
Bodas, Dhananjay, IMTEK, Germany
Borges Carval, Nuno, Universidade de Aveiro, Portugal
Bousbia-Salah, Mounir, University of Annaba, Algeria
Bouvet, Marcel, CNRS – UPMC, France
Brudzewski, Kazimierz, Warsaw University of Technology, Poland
Cai, Chenxin, Nanjing Normal University, China
Cai, Qingyun, Hunan University, China
Campanella, Luigi, University La Sapienza, Italy
Carvalho, Vitor, Minho University, Portugal
Cecelja, Franjo, Brunel University, London, UK
Cerda Belmonte, Judith, Imperial College London, UK
Chakrabarty, Chandan Kumar, Universiti Tenaga Nasional, Malaysia
Chakravorty, Dipankar, Association for the Cultivation of Science, India
Changhai, Ru, Harbin Engineering University, China
Chaudhari, Gajanan, Shri Shivaji Science College, India
Chen, Rongshun, National Tsing Hua University, Taiwan
Cheng, Kuo-Sheng, National Cheng Kung University, Taiwan
Chiriac, Horia, National Institute of Research and Development, Romania
Chowdhuri, Arijit, University of Delhi, India
Chung, Wen-Yaw, Chung Yuan Christian University, Taiwan
Corres, Jesus, Universidad Publica de Navarra, Spain
Cortes, Camilo A., Universidad de La Salle, Colombia
Courtois, Christian, Universite de Valenciennes, France
Cusano, Andrea, University of Sannio, Italy
D'Amico, Arnaldo, Università di Tor Vergata, Italy
De Stefano, Luca, Institute for Microelectronics and Microsystem, Italy
Deshmukh, Kiran, Shri Shivaji Mahavidyalaya, Barshi, India
Kang, Moonho, Sunmoon University, Korea South
Kaniusas, Eugenijus, Vienna University of Technology, Austria
Katake, Anup, Texas A&M University, USA
Dickert, Franz L., Vienna University, Austria
Dieguez, Angel, University of Barcelona, Spain
Dimitropoulos, Panos, University of Thessaly, Greece
Ding Jian, Ning, Jiangsu University, China
Djordjevic, Alexandar, City University of Hong Kong, Hong Kong
Donato, Nicola, University of Messina, Italy
Donato, Patricio, Universidad de Mar del Plata, Argentina
Dong, Feng, Tianjin University, China
Drljaca, Predrag, Instersema Sensoric SA, Switzerland
Dubey, Venketesh, Bournemouth University, UK
Enderle, Stefan, University of Ulm and KTB mechatronics GmbH, Germany
Erdem, Gursan K. Arzum, Ege University, Turkey
Erkmen, Aydan M., Middle East Technical University, Turkey
Estelle, Patrice, Insa Rennes, France
Estrada, Horacio, University of North Carolina, USA
Faiz, Adil, INSA Lyon, France
Fericean, Sorin, Balluff GmbH, Germany
Fernandes, Joana M., University of Porto, Portugal
Francioso, Luca, CNR-IMM Institute for Microelectronics and Microsystems, Italy
Fu, Weiling, South-Western Hospital, Chongqing, China
Gaura, Elena, Coventry University, UK
Geng, Yanfeng, China University of Petroleum, China
Gole, James, Georgia Institute of Technology, USA
Gong, Hao, National University of Singapore, Singapore
Gonzalez de la Ros, Juan Jose, University of Cadiz, Spain
Granell, Annette, Goteborg University, Sweden
Graff, Mason, The University of Texas at Arlington, USA
Guan, Shan, Eastman Kodak, USA
Guillet, Bruno, University of Caen, France
Guo, Zhen, New Jersey Institute of Technology, USA
Gupta, Narendra Kumar, Napier University, UK
Hadjiloucas, Sillas, The University of Reading, UK
Hashsham, Syed, Michigan State University, USA
Hernandez, Alvaro, University of Alcalá, Spain
Hernandez, Wilmar, Universidad Politecnica de Madrid, Spain
Homentcovschi, Dorel, SUNY Binghamton, USA
Horstman, Tom, U.S. Automation Group, LLC, USA
Hsiai, Tzung (John), University of Southern California, USA
Huang, Jeng-Sheng, Chung Yuan Christian University, Taiwan
Huang, Star, National Tsing Hua University, Taiwan
Huang, Wei, PSG Design Center, USA
Hui, David, University of New Orleans, USA
Jaffrezic-Renault, Nicole, Ecole Centrale de Lyon, France
Jaime Calvo-Galleg, Jaime, Universidad de Salamanca, Spain
James, Daniel, Griffith University, Australia
Janting, Jakob, DELTA Danish Electronics, Denmark
Jiang, Liudi, University of Southampton, UK
Jiao, Zheng, Shanghai University, China
John, Joachim, IMEC, Belgium
Kalach, Andrew, Voronezh Institute of Ministry of Interior, Russia
Rodriguez, Angel, Universidad Politecnica de Cataluna, Spain
Rothberg, Steve, Loughborough University, UK

Kausel, Wilfried, University of Music, Vienna, Austria
Kavasoglu, Nese, Mugla University, Turkey
Ke, Cathy, Tyndall National Institute, Ireland
Khan, Asif, Aligarh Muslim University, Aligarh, India
Kim, Min Young, Koh Young Technology, Inc., Korea South
Ko, Sang Choon, Electronics and Telecommunications Research Institute, Korea South
Kockar, Hakan, Balikesir University, Turkey
Kotulska, Malgorzata, Wroclaw University of Technology, Poland
Kratz, Henrik, Uppsala University, Sweden
Kumar, Arun, University of South Florida, USA
Kumar, Subodh, National Physical Laboratory, India
Kung, Chih-Hsien, Chang-Jung Christian University, Taiwan
Lacnjevac, Caslav, University of Belgrade, Serbia
Laurent, Francis, IMEC, Belgium
Lay-Ekuakille, Aime, University of Lecce, Italy
Lee, Jang Myung, Pusan National University, Korea South
Lee, Jun Su, Amkor Technology, Inc. South Korea
Lei, Hua, National Starch and Chemical Company, USA
Li, Genxi, Nanjing University, China
Li, Hui, Shanghai Jiaotong University, China
Li, Xian-Fang, Central South University, China
Liang, Yuanchang, University of Washington, USA
Liawruangrath, Saisunee, Chiang Mai University, Thailand
Liew, Kim Meow, City University of Hong Kong, Hong Kong
Lin, Hermann, National Kaohsiung University, Taiwan
Lin, Paul, Cleveland State University, USA
Linderholm, Pontus, EPFL - Microsystems Laboratory, Switzerland
Liu, Aihua, Michigan State University, USA
Liu Changgeng, Louisiana State University, USA
Liu, Cheng-Hsien, National Tsing Hua University, Taiwan
Liu, Songqin, Southeast University, China
Lodeiro, Carlos, Universidade NOVA de Lisboa, Portugal
Lorenzo, Maria Encarnacio, Universidad Autonoma de Madrid, Spain
Lukaszewicz, Jerzy Pawel, Nicholas Copernicus University, Poland
Ma, Zhanfang, Northeast Normal University, China
Majstorovic, Vidosav, University of Belgrade, Serbia
Marquez, Alfredo, Centro de Investigacion en Materiales Avanzados, Mexico
Matay, Ladislav, Slovak Academy of Sciences, Slovakia
Mathur, Prafull, National Physical Laboratory, India
Maurya, D.K., Institute of Materials Research and Engineering, Singapore
Mekid, Samir, University of Manchester, UK
Mendes, Paulo, University of Minho, Portugal
Mennell, Julie, Northumbria University, UK
Mi, Bin, Boston Scientific Corporation, USA
Minas, Graca, University of Minho, Portugal
Moghavvemi, Mahmoud, University of Malaya, Malaysia
Mohammadi, Mohammad-Reza, University of Cambridge, UK
Molina Flores, Esteban, Benemirita Universidad Autonoma de Puebla, Mexico
Moradi, Majid, University of Kerman, Iran
Morello, Rosario, DIMET, University "Mediterranea" of Reggio Calabria, Italy
Mounir, Ben Ali, University of Sousse, Tunisia
Mukhopadhyay, Subhas, Massey University, New Zealand
Neelamegam, Periasamy, Sastra Deemed University, India
Neshkova, Milka, Bulgarian Academy of Sciences, Bulgaria
Oberhammer, Joachim, Royal Institute of Technology, Sweden
Ould Lahoucine, University of Guelma, Algeria
Pamidighanta, Sayanu, Bharat Electronics Limited (BEL), India
Pan, Jisheng, Institute of Materials Research & Engineering, Singapore
Park, Joon-Shik, Korea Electronics Technology Institute, Korea South
Pereira, Jose Miguel, Instituto Politecnico de Seteбал, Portugal
Petsev, Dimitar, University of New Mexico, USA
Pogacnik, Lea, University of Ljubljana, Slovenia
Post, Michael, National Research Council, Canada
Prance, Robert, University of Sussex, UK
Prasad, Ambika, Gulbarga University, India
Prateepasen, Asa, Kingmoungut's University of Technology, Thailand
Pullini, Daniele, Centro Ricerche FIAT, Italy
Pumera, Martin, National Institute for Materials Science, Japan
Radhakrishnan, S., National Chemical Laboratory, Pune, India
Rajanna, K., Indian Institute of Science, India
Ramadan, Qasem, Institute of Microelectronics, Singapore
Rao, Basuthkar, Tata Inst. of Fundamental Research, India
Reig, Candid, University of Valencia, Spain
Restivo, Maria Teresa, University of Porto, Portugal
Rezazadeh, Ghader, Urmia University, Iran
Robert, Michel, University Henri Poincare, France
Royo, Santiago, Universitat Politecnica de Catalunya, Spain
Sadana, Ajit, University of Mississippi, USA
Sandacci, Serghei, Sensor Technology Ltd., UK
Sapozhnikova, Ksenia, D.I.Mendeleyev Institute for Metrology, Russia
Saxena, Vibha, Bhabha Atomic Research Centre, Mumbai, India
Schneider, John K., Ultra-Scan Corporation, USA
Seif, Selemeni, Alabama A & M University, USA
Seifter, Achim, Los Alamos National Laboratory, USA
Sengupta, Deepak, Advance Bio-Photonics, India
Shearwood, Christopher, Nanyang Technological University, Singapore
Shin, Kyuho, Samsung Advanced Institute of Technology, Korea
Shmaliy, Yuriy, Kharkiv National University of Radio Electronics, Ukraine
Silva Girao, Pedro, Technical University of Lisbon Portugal
Slomovitz, Daniel, UTE, Uruguay
Smith, Martin, Open University, UK
Soleymanpour, Ahmad, Damghan Basic Science University, Iran
Somani, Prakash R., Centre for Materials for Electronics Technology, India
Srinivas, Talabattula, Indian Institute of Science, Bangalore, India
Srivastava, Arvind K., Northwestern University
Stefan-van Staden, Raluca-Ioana, University of Pretoria, South Africa
Sumriddetchka, Sarun, National Electronics and Computer Technology Center, Thailand
Sun, Chengliang, Polytechnic University, Hong-Kong
Sun, Dongming, Jilin University, China
Sun, Junhua, Beijing University of Aeronautics and Astronautics, China
Sun, Zhiqiang, Central South University, China
Suri, C. Raman, Institute of Microbial Technology, India
Sysoev, Victor, Saratov State Technical University, Russia
Szewczyk, Roman, Industrial Research Institute for Automation and Measurement, Poland
Tan, Ooi Kiang, Nanyang Technological University, Singapore
Tang, Dianping, Southwest University, China
Tang, Jaw-Luen, National Chung Cheng University, Taiwan
Thumbavanam Pad, Kartik, Carnegie Mellon University, USA
Tsiantos, Vassilios, Technological Educational Institute of Kaval, Greece
Tsigara, Anna, National Hellenic Research Foundation, Greece
Twomey, Karen, University College Cork, Ireland
Valente, Antonio, University, Vila Real, - U.T.A.D., Portugal
Vaseashta, Ashok, Marshall University, USA
Vazques, Carmen, Carlos III University in Madrid, Spain
Vieira, Manuela, Instituto Superior de Engenharia de Lisboa, Portugal
Vigna, Benedetto, STMicroelectronics, Italy
Vrba, Radimir, Brno University of Technology, Czech Republic
Wandelt, Barbara, Technical University of Lodz, Poland
Wang, Jiangping, Xi'an Shiyou University, China
Wang, Kedong, Beihang University, China
Wang, Liang, Advanced Micro Devices, USA
Wang, Mi, University of Leeds, UK
Wang, Shinn-Fwu, Ching Yun University, Taiwan
Wang, Wei-Chih, University of Washington, USA
Wang, Wensheng, University of Pennsylvania, USA
Watson, Steven, Center for NanoSpace Technologies Inc., USA
Weiping, Yan, Dalian University of Technology, China
Wells, Stephen, Southern Company Services, USA
Wolkenberg, Andrzej, Institute of Electron Technology, Poland
Woods, R. Clive, Louisiana State University, USA
Wu, DerHo, National Pingtung University of Science and Technology, Taiwan
Wu, Zhaoyang, Hunan University, China
Xiu Tao, Ge, Chuzhou University, China
Xu, Tao, University of California, Irvine, USA
Yang, Dongfang, National Research Council, Canada
Yang, Wuqiang, The University of Manchester, UK
Ymeti, Aurel, University of Twente, Netherland
Yu, Haihu, Wuhan University of Technology, China
Yufera Garcia, Alberto, Seville University, Spain
Zagnoni, Michele, University of Southampton, UK
Zeni, Luigi, Second University of Naples, Italy
Zhong, Haoxiang, Henan Normal University, China
Zhang, Minglong, Shanghai University, China
Zhang, Qintao, University of California at Berkeley, USA
Zhang, Weiping, Shanghai Jiao Tong University, China
Zhang, Wenming, Shanghai Jiao Tong University, China
Zhou, Zhi-Gang, Tsinghua University, China
Zorzano, Luis, Universidad de La Rioja, Spain
Zourob, Mohammed, University of Cambridge, UK

Contents

Volume 85
Issue 11
November 2007

www.sensorsportal.com

ISSN 1726-5479

Research Articles

Optical Characterization of the Interaction of Mercury with Nanoparticulate Gold Suspended in Solution <i>Kevin Scallan, Donald Lucas, and Catherine Koshland</i>	1687
Electrical Characterization of a Nanoporous Silicon Sensor for Low ppm Gas Moisture Sensing <i>Tarikul Islam, Hiranmay Saha</i>	1699
Focused Ion Beam Nanopatterning for Carbon Nanotube Ropes based Sensor <i>Vera La Ferrara, Ivana Nasti, Brigida Alfano, Ettore Massera and Girolamo Di Francia</i>	1708
Trace Moisture Response Property of Thin Film Nano Porous γ-Al₂O₃ for Industrial Application <i>Debdulal Saha, Kamalendu Sengupta</i>	1714
Gas Detectors Based on Single Wall Carbon Nanotubes by Exploiting the Dielectrophoresis Method <i>Lun-Wei Chang and Juh-Tzeng Lue</i>	1721
Detection of Hydrogen Sulphide Gas Sensor Based Nanostructured Ba₂CrMoO₆ Thick Films <i>A. V. Kadu, N. N. Gedam and G. N. Chaudhari</i>	1728
Nanocomposites Sn-Si-O and Sn-Mn-O for Gas Sensors <i>Ekaterina Rembeza, Stanislav Rembeza</i>	1739
Theory and Instrumentation Related to Anomalous Dielectric Dispersion in Ordered Molecular Groups <i>Tanmoy Maity, D. Ghosh and C. R. Mahata</i>	1745
Flexible Membrane Impact Sensor via Thick Film Method <i>Hee C. Lim, James Zunino III and John F. Federici</i>	1757
Humidity Sensing Behaviour of Niobium Oxide: Primitive Study <i>B. C. Yadav, Richa Srivastava, M. Singh, R. Kumar and C. D. Dwivedi</i>	1765

Authors are encouraged to submit article in MS Word (doc) and Acrobat (pdf) formats by e-mail: editor@sensorsportal.com
Please visit journal's webpage with preparation instructions: <http://www.sensorsportal.com/HTML/DIGEST/Submission.htm>

Optical Characterization of the Interaction of Mercury with Nanoparticulate Gold Suspended in Solution

¹Kevin SCALLAN, ²Donald LUCAS, and ³Catherine KOSHLAND

¹Department of Mechanical Engineering, University of California at Berkeley,

²Environmental Energy Technologies Division, Lawrence Berkeley National Laboratory,

³School of Public Health, University of California at Berkeley, Berkeley, CA 94720

Tel: +1-510-486 4134

E-mail: kscallan@me.berkeley.edu

Received: 27 February 2007 / Accepted: 20 November 2007 / Published: 26 November 2007

Abstract: We have demonstrated that the surface plasmon resonance (SPR) wavelength of gold nanoparticles suspended in solution can be modified by exposure to elemental mercury at sub parts per million (ppm) concentrations in nitrogen. Ultraviolet-visible (UV-vis) absorption spectroscopy was used to monitor the wavelength and maximum absorbance of the colloidal solution during and after the exposure process. Transmission electron microscopy (TEM) images revealed modifications to the morphology of the particles (size, shape, and extent of aggregation). The results show that the SPR wavelength is blue-shifted and the absorbance is increased with exposure time. After the exposure, the spectra were observed to relax toward their original position suggesting that the detection medium is regenerative. *Copyright © 2007 IFSA.*

Keywords: Mercury, Gold, Nanoparticle, Surface plasmon resonance

1. Introduction

The detection and quantification of mercury are important in many applications including environmental monitoring, waste management, developmental biology, and clinical toxicology. Because of its persistent, bioaccumulative, and toxic (PBT) nature, mercury contamination has emerged as a global concern. Elemental mercury, given its high vapor pressure (1.6 ppm on a mass basis at standard temperature and pressure, [1a]), high diffusivity in air (0.135 ± 0.003 cm²/s, [2]), low water solubility (50 ppb on a mass basis at STP, [3]), and relative stability is difficult to capture, can be transported long distances, and has an atmospheric residence time of between 1-2 years.

Gaseous (elemental) mercury is the dominant atmospheric species [4, 5]. It is removed from the atmosphere by dry deposition onto surfaces or by wet deposition after oxidation to water-soluble monovalent or divalent mercury. Divalent mercury is more stable and thus more common in the atmosphere, and is typically the primary component in oxic, suboxic, and anoxic aqueous environments [6]. It can be associated with inorganic molecules including chlorine, sulfur, and hydroxyl ions, and organic molecules giving rise to monomethylmercury and dimethylmercury, both of which are highly toxic and can bioaccumulate by up to a factor of 10^5 in the aquatic food chain [7]. Monomethylmercury is the most significant species in terms of adverse biological effects but typically only represents a small fraction of the total mercury in any medium. However, given that all species of mercury can be converted to the monomethyl compound, a quantitative understanding of the environmental fate of the species is critical to controlling, regulating, and assessing the ecological risk of mercury contamination. In particular, the control and regulation of gaseous or elemental mercury is of fundamental importance. The primary source of elemental mercury is anthropogenic emissions from coal-fired power plants and waste incineration facilities [8]. Recently, new regulation aimed at minimizing the human health effects and environmental hazards caused by mercury pollution has necessitated the need for sensitive, reliable, portable, and inexpensive mercury detectors [9].

Commercial mercury analyzers are primarily based on atomic absorption spectroscopy, atomic fluorescence spectroscopy, or inductively coupled plasma mass spectrometry. These techniques, while sensitive, generally lack portability, are expensive, and often require analyte preconcentration onto the surface of a noble metal. In principle, colorimetric methods have the potential to satisfy the requirements for a simple, real-time, portable continuous mercury emissions analyzer but given that most conventional molecular dyes exhibit relatively low extinction coefficients, the challenge is to identify appropriate binding leuco dyes capable of yielding sufficiently intense absorbing metal/dye complexes [10]. An alternative is to use nonmolecular chromophores such as free-electron metal nanoparticles that display visible extinction coefficients up to several orders of magnitude higher, e.g.: gold, silver, and copper.

In this paper, we demonstrate the potential for a sensitive, reliable, portable, inexpensive elemental mercury detector that takes advantage of the visible surface plasmon resonance (SPR) wavelength of gold nanoparticles. We first hypothesized that the SPR phenomenon can be used as an analytical tool to detect and quantify the concentration of elemental mercury adsorbed and/or absorbed to gold nanoparticles suspended in solution. Aqueous suspensions of the gold particles display an intense plasmon absorption band centered at approximately 520 nm that renders the colloidal solution ruby-red in color. Gold nanoparticles were chosen for a number of reasons. First, as is well known in the mining industry, mercury has a high affinity for gold and will readily form an amalgam [11]. Second, gold nanoparticles display a surface plasmon resonance (SPR) band in the visible region at about 520 nm. The exact location of the SPR wavelength is a complex function of particle morphology, the surrounding medium, and any adsorbent species present [12, 13]. By maintaining a constant particle size and shape, and stable surrounding medium, the degree to which a particular adsorbent, for example elemental mercury, is adsorbed by the particles can be directly related to the change in the SPR wavelength. A further advantage of using gold nanoparticles is their very high surface area to volume ratio which minimizes the amount of material required and maximizes the sensitivity.

2. Material and Methods

Colloidal gold was procured from British Biocell International (BBI), product code EM.GC5. The particle diameter was 5 nm with coefficient of variation $< 15\%$ (0.75 nm) and particle roundness greater than 95%. The particle concentration was calculated to be 5×10^{13} particles per ml with a molar absorptivity of $2058 \text{ M}^{-1} \text{ cm}^{-1}$ at the SPR peak. The solution was stored in a transparent, polyethylene terephthalate (PETE) container at room temperature and remained stable for the duration

of the experiment. Elemental mercury (99.9999% electronic grade from Aldrich Chem. Co.) was used as the source of mercury vapor.

The experimental apparatus is shown in Fig. 1. A bead (1 gram) of elemental mercury was indirectly submerged into a temperature controlled water bath and its vapor pressure controlled by setting the temperature of the bath. The mercury vapor was entrained in a nitrogen (99.999% from Airgas) carrier stream flowing at 140 cubic centimeters per minute (ccm) and was assumed to be in a state of equilibrium. The mercury vapor was exposed to the gold nanoparticles by bubbling the carrier stream through a series of three 4 ml UV-vis cuvettes with a 1 cm path length. Each cuvette contained 3.2 ml of the colloidal gold solution.

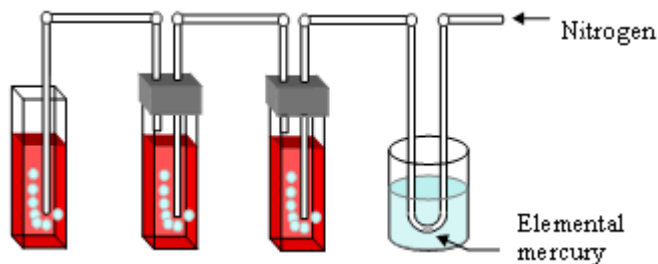


Fig. 1. The experimental apparatus consisting of three cuvettes, a water bath to control the temperature, and a bead of elemental mercury. The carrier stream was permitted to escape from the system after the last cuvette (i.e. #3, the left most cuvette).

The experimental apparatus enabled us to relate the sensitivity of changes in the SPR wavelength to the amount of mercury bubbled through the system, and to quantify the capture efficiency (defined as the ratio of the number of mercury atoms captured by the colloidal solution to the total number of atoms bubbled through the solution).

3. Characterization

A Perkin Elmer Lambda 2 UV-vis spectrometer was used to record the absorption spectra of the colloidal solutions during and after the exposure. Standard 1 x 1 x 4 cm³ high density polyethylene (HDPE) UV-vis cuvettes were used and the background was set to pure (18.2 MΩ.cm) ambient temperature distilled water from a Millipore Milli-Q[®] ultrapure water purification system connected in series with a Barnstead Fi-Stream[®] type II distillation glass still. A FEI model Technai 12 TEM was used to image the particles. The TEM samples were prepared on carbon coated 200 square-mesh TEM grids (from SPI Supplies) by allowing a drop of the colloidal solution to dry by evaporation from the grid surface.

4. Results and Discussion

The samples were characterized by UV-vis absorption spectroscopy and TEM imaging. Fig. 2(a) shows the UV-vis spectrum of the colloidal solution, as received. A TEM image of the particles is shown in Fig. 2(b). The broad absorption band centered at 519 nm (2.4 eV) is a result of the collective oscillation of free conduction electrons in response to an electromagnetic field [13-16]. The position and width of the band depends on several factors including single particle properties (e.g. surface functionality, adsorbate effects, electron density, etc.), the refractive index and viscosity of the surrounding medium, particle concentration or average distance between neighboring particles, and

temperature [12,13]. Provided these variables are known, the position of the resonance band maximum can be used to assess colloidal concentration and particle size in solution [17].

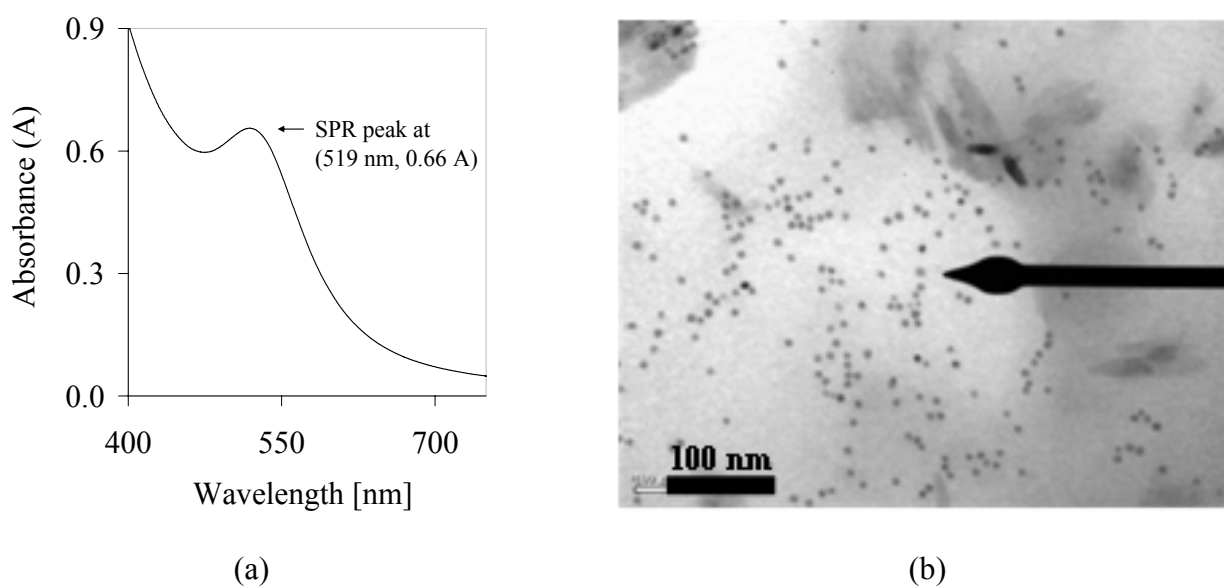


Fig. 2. (a) UV-vis absorption spectrum of the colloidal gold solution illustrating the SPR peak at 519 nm. The absorbance at the SPR peak is 0.66 A. (b) TEM image of the colloidal particles – the scale bar reads 100 nm.

4.1. The Surface Plasmon Resonance Phenomenon

The SPR effect was first described quantitatively by classical electrodynamic (Mie) theory, based on bulk optical properties, by solving Maxwell's equations with appropriate boundary conditions for small (< 100 nm) spherical particles [18]. For nanoparticles that are small compared to the wavelength of the exciting electromagnetic radiation ($2R \ll \lambda$, $2R < 25$ nm for gold [15]) the quasi-static or discrete dipole approximation can be used and the extinction (absorption plus scattering) cross section is given by [13, 14, 19]:

$$\sigma(\omega) = 9V_o \varepsilon_m^{3/2} \frac{\omega}{c} \frac{\varepsilon''}{[\varepsilon' + 2\varepsilon_m]^2 + \varepsilon''^2}, \quad (1)$$

where V_o is the spherical particle volume, c is the speed of light, ω is the angular frequency of the exciting radiation, ε_m the dielectric constant of the surrounding medium (assumed to be frequency independent) and ε' and ε'' are the real and imaginary parts of the complex dielectric function of the particle material respectively. From (1), Mie theory predicts that the surface plasmon resonance band occurs when $\varepsilon' \approx -2\varepsilon_m$ (i.e., at the Fröhlich frequency) provided ε'' is small and only weakly dependent on the frequency. Further, (1) predicts that the position and width of the plasmon band are determined solely by ε'' and are independent of size, except for a varying intensity due to the volume term.

In practice, however, a clear size-dependence is observed [13, 14, 20-23]. To account for these findings, basic Mie theory has evolved to include the fundamental assumption that the dielectric function of the nanoparticle material is size dependent (i.e. the intrinsic size-effect). The need to introduce this size-dependence has been proposed to occur for free-electron metal particles when their size becomes smaller than the electronic mean free path in the bulk metal, approximately 20 nm for gold [13]. Using (1) and the bulk optical properties of gold [1b], the UV-vis spectrum of five differently sized colloidal gold particles suspended in water was calculated. The spectra, normalized to

one at the SPR wavelength, are shown in Fig. 3(a). For reasons not fully justified (see [22], p. 162), only the imaginary component of the particle dielectric function was adjusted for size (following the method of Hovel *et al.* [24]). The result is a $1/R$ dependence of the plasmon bandwidth on particle size, in agreement with experimental results, and a fixed SPR wavelength.

For larger particles, the extinction cross section is also size dependent and is accurately described by the full Mie equation. The size-dependence is a result of changes to the real part of the dielectric component of the particle material. In general, ϵ' is an increasing function of frequency; when the particle size is increased the absorption maximum is red-shifted. This is known as the extrinsic size-effect and is used extensively in the sizing of metal particles by optical extinction spectroscopy [22]. Shown in Fig. 3(b) are the normalized extinction cross sections of four differently sized gold nanoparticles suspended in water. The spectra were calculated using the full Mie equation, the numerical code in Bohren & Huffman ([16], Appendix A), and bulk optical properties. Clearly, the plasmon bandwidth increases and the position of the SPR peak red-shifts with increasing particle size. Below 10 nm the spectra were identical, hence the need to introduce the intrinsic size-effect.

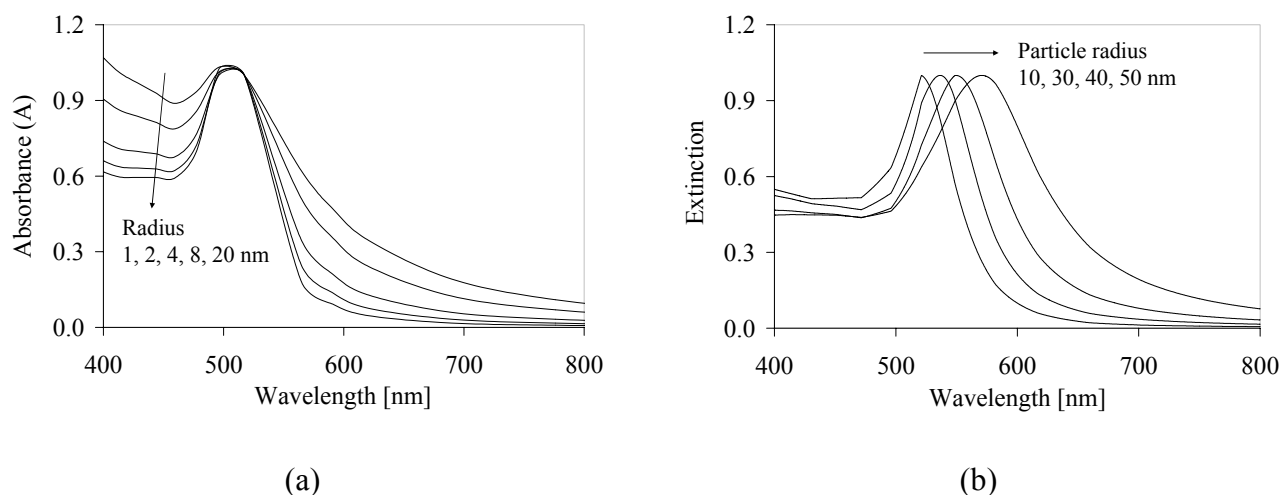


Fig. 3. (a) Calculated UV-vis absorption spectra of five different sized colloidal gold particles suspended in water using equation (1). Only the imaginary part of the dielectric function of the particle material was adjusted for size (see Scaffardi *et al.* 2005). (b) Calculated UV-vis extinction spectra of four different sized colloidal gold particles suspended in water using full Mie theory.

Bohren and Huffman [16] also considered the case of small, homogeneous spheres uniformly coated with a mantle of different composition. The effect of the coating was to shift the Fröhlich frequency. The magnitude of the shift was determined to be a function of the real part of the dielectric function of the sphere as well as the kind and amount of coating. For the purpose of this work, it is important to note that the position of the SPR peak is expected to be a function of particle size and single particle properties.

4.2 Experiment

The concentration of mercury in the carrier stream was controlled by setting the temperature of the mercury source. Three vapor pressures were considered (a) 0.215 ± 0.035 ppm, (b) 1.6 ± 0.01 ppm, and (c) 81 ± 9 ppm mercury in nitrogen corresponding to a mercury source (water bath) temperature of 0 °C, 20 °C, and 80 °C respectively. The vapor pressures were calculated using data (section 12-131) tabulated in the CRC Handbook of Chemistry and Physics [1] and compared with previously

reported values for consistency and accuracy [2, 6, 25]. The real UV-vis absorption spectra of the colloidal solutions as a function of exposure time for case (b) are shown in Fig. 4. In each case, the SPR wavelength was observed to blue-shift and the absorbance increased as the total quantity of mercury bubbled through the system increased. Table 1 shows the magnitude of the blue-shift and the increase in absorbance (both measured from the original surface plasmon maximum) as a function of time. Both the shift in the wavelength and change in absorbance were significant; however given that the molar absorptivity at a particular wavelength is constant regardless of the particle concentration (i.e. Beer's law), the shift in the wavelength was chosen as the most appropriate metric to quantify the changes induced by the mercury.

After one hour of exposure, the blue-shift for cases (a), (b), and (c) was 8 nm, 22 nm, and 34 nm respectively. The SPR wavelength moved approximately linearly with exposure time except for case (a) cuvette #3 and case (c) cuvette #1. In case (a), the extremely low concentration ($\ll 0.215$ ppm) of mercury flowing through the solution in cuvette #3 is the most probable explanation for the non-linear response. In case (c), the alternative is likely true. The high concentration (c. 81 ppm) of mercury flowing through cuvette #1 was such that the solution saturated at short exposure times and yielded no further wavelength-shift. The best fit, most linear response was obtained for case (c) cuvette #1. In this sample, the blue-shift fitted the linear regression equation $0.132\tau - 0.04$ (where τ is the exposure time) with an R-square value equal to 0.99. Given that the maximum solubility of mercury in water (16.9 $\mu\text{g/L}$ at 21 °C, [26, 27]) is much greater than the actual amount of mercury bubbled through the system, it can be inferred that it is the exterior and/or interior of the gold particles that become saturated and not the surrounding medium. Further, Miller *et al.* [26] have observed that it can take on the order of months for a water medium to become saturated with mercury even when there is sufficient mercury to saturate the stream. Thus, provided (i) there is sufficient mercury flowing through the system, (ii) the solution is not overwhelmed or saturated with mercury, and (iii) the original location of the SPR maximum is known, the extent of the blue-shift can be used to quantify the amount of mercury flowing through the system. It remains to be investigated whether a similar, linear type of relationship holds true for other types of colloidal gold (e.g., thiocyanate, sodium borohydride, sodium citrate, 4-dimethyl-aminopyridine DMAP, etc.).

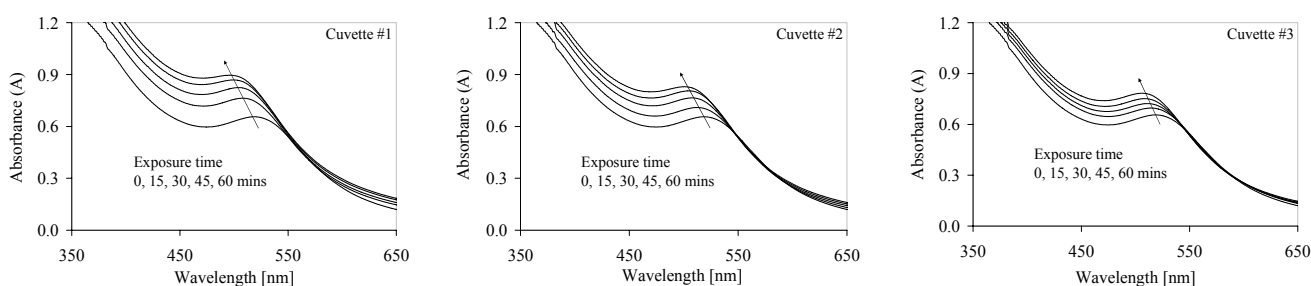


Fig. 4. Case (b). UV-vis spectra of the three colloidal solutions after exposure to 1.6 ppm mercury in nitrogen as a function of exposure time in minutes.

Considering the free-electron theory, the SPR wavelength is also proportional to the inverse square root of the electron density $N^{-1/2}$ (see Morris [27]). Thus, an increase in electron density due to mercury adsorption should give rise to a decrease in the SPR wavelength. Fig. 10 shows that the predicted relationship is true provided the same conditions prescribed above are satisfied, i.e. (i) there is sufficient mercury flowing through the system such that a linear relationship can be established (i.e., enough mercury to interact with the entire medium) and (ii) the solution is not saturated with mercury. The increase in electron density due to the mercury exposure was calculated from the equation:

$$N = \frac{\tau Q N_A}{(1 \times 10^9)} \left(\frac{C v}{M} \right)_{Hg}, \quad (2)$$

where τ is the exposure time in minutes, Q is the flowrate (140 cm³/min), N_A is Avogadro's number, C_{Hg} is the concentration of mercury in the carrier stream expressed in ng/cm³, v_{Hg} is the number of valence (conduction-band) electrons per mercury atom (i.e. two), and M_{Hg} the molar mass of mercury. Fig. 6 shows the relationship between the increase in electron density (expressed in terms of the exposure time in minutes) and the SPR wavelength for case (c). For cuvette #1, the solution began to saturate after approx. 15 min. The experimental data fitted a parabolic regression curve with near perfect accuracy (R-square value of 0.99). At lower concentrations – cuvettes #2 and #3 – the data fitted a linear regression as predicted by (2) (R-square value of 0.99 in both cases).

Table 1. The blue-shift in nm (left) and increase in absorbance (right) as a function of exposure time each case. Both the blue-shift and change in absorbance were calculated from the original surface plasmon resonance maximum position.

		Case	Cuvette	15 mins	30 mins	45 mins	60 mins			Case	Cuvette	15 mins	30 mins	45 mins	60 mins
Blue-shift [nm]	(a)	#1		2.0	3.8	5.8	8.0	Δ Absorbance (A)	(a)	#1		0.007	0.002	0.052	0.072
		#2		1.6	2.0	3.8	4.2			#2		0.005	0.014	0.029	0.038
		#3		0.2	1.8	2.0	2.0			#3		0.013	0.022	0.029	0.031
	(b)	#1		9.8	14.0	19.6	22.0		(b)	#1		0.108	0.169	0.213	0.241
		#2		6.0	10.0	14.0	17.8			#2		0.054	0.109	0.150	0.174
		#3		3.8	7.8	9.6	12.0			#3		0.040	0.067	0.096	0.128
	(c)	#1		16.0	26.0	32.0	34.0		(c)	#1		0.142	0.194	0.219	0.241
		#2		8.2	14.2	20.0	25.8			#2		0.723	0.784	0.819	0.822
		#3		6.0	9.8	14.0	19.8			#3		0.044	0.085	0.136	0.196

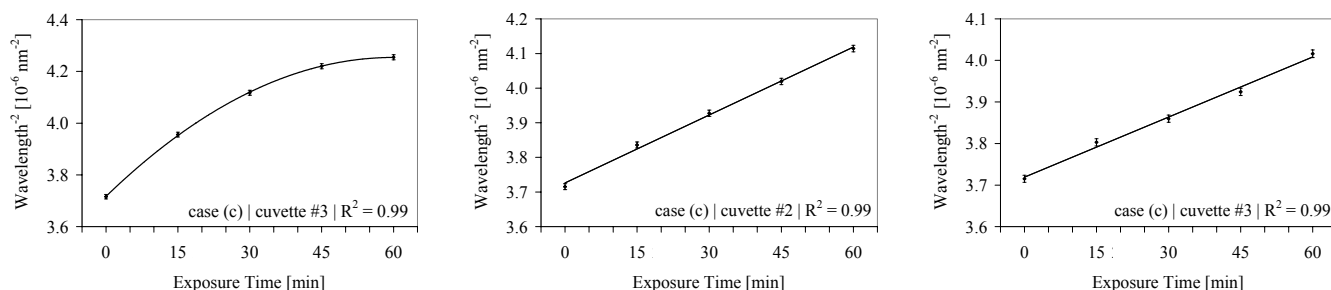


Fig. 6. Case (c): Relationship between the SPR wavelength and the increase in electron density (expressed in terms of the exposure time in minutes). The error bars represent a 0.3 nm variation in the wavelength readings.

4.3 Detection Limit

To calculate a detection limit (DL), a number of factors were considered. First, the time needed to respond, record, and analyze the data, and second the wavelength accuracy of the UV-vis spectrometer. For a 2 sec response time (a function of the UV-vis spectrometer), a scan-speed of 240 nm over a 50 nm range (approximate range needed to detect a change), and an estimated analysis time of 30 sec, the detection time is estimated to be approximately 45 sec. It is shown below that the detection time does not place any constraints on the detection limit.

The wavelength accuracy of the UV-vis spectrometer was 0.3 nm. Shown in Fig. 7 is the relationship between the increase in electron density and the SPR wavelength for case (a). As the concentration of

mercury is decreased, the blue-shift, and the slope of the relationship between the SPR wavelength and the increase in electron density also decrease (cf. with Fig. 6). Below a certain mercury concentration, the error in the wavelength becomes significant. For case (a), cuvette #1, a linear relationship with regression coefficient or slope equal to 0.0019 was observed and none of the error bars overlapped. For cuvettes #2 and #3 (regression coefficient of 0.0010 and 0.0006 respectively), significant overlap occurred. Accordingly, the wavelength accuracy of the spectrometer was insufficient to detect changes in the SPR wavelength at such concentrations. It follows that the DL lies between the concentration of mercury flowing through cuvettes #1 and #2. A conservative estimate is 0.215 ± 0.035 ppm, i.e. the concentration of mercury flowing through cuvette #1. By taking the relative shift in the wavelength as a suitable metric for quantifying the amount of mercury exposed to the solution, the concentration of mercury flowing through cuvette #2 can be calculated. After 60 minutes, the blue-shift in cuvette #2 (4.2 nm) was 52.5% that in cuvette #3 (8.0 nm). Hence, it can be inferred that the concentration of mercury flowing through cuvette #2 was 52.5% that in cuvette #3. Stated another way, approximately 47.5% of the mercury atoms flowing through cuvette #1 were captured (i.e. adsorbed and/or absorbed) by the gold nanoparticles in solution. Taking the average of the two concentrations yields a DL of approximately 0.16 ppm (1.3 ng/cm^3).

It is important to note that there is considerable scope to lower this DL. Commercial, high resolution (HR) portable UV-vis spectrometers are readily available. Take for example the HR4000 Spectrometer from Ocean Optics, Inc. This miniature ($145 \times 104 \text{ mm}^2$ footprint) spectrometer utilizes a 3648 element CCD array detector (from Toshiba) and achieves an optical resolution of 0.02 nm. Such a device has the potential to lower the DL by two orders of magnitude and thus yield ppb sensitivity. The DL could also be lowered by increasing the path length and/or by bubbling the carrier stream through the colloidal solutions for longer times.

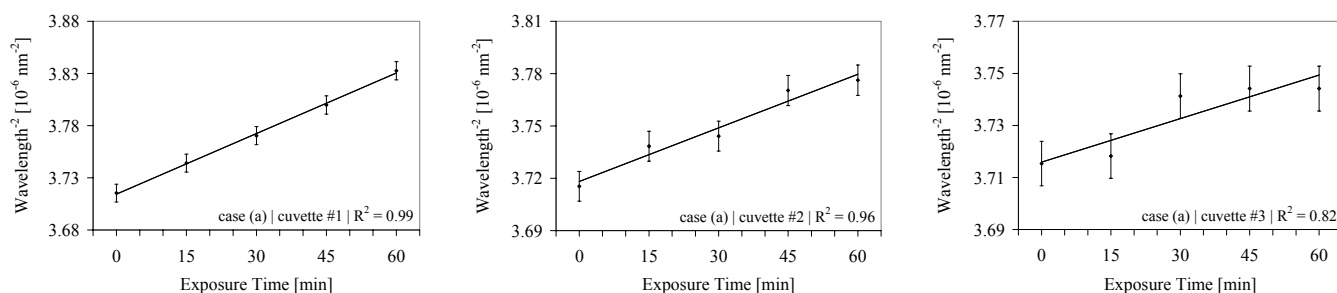


Fig. 7. Case (a): Relationship between the SPR wavelength and the increase in electron density (expressed in terms of the exposure time in minutes). The linear regression coefficient of determination or R-square value is 0.99, 0.96, and 0.82 for cuvettes #1, #2, and #3 respectively. The error bars represent a 0.3 nm variation in the wavelength readings and are a function of the accuracy of the UV-vis spectrometer.

The number of mercury atoms per particle was calculated to estimate (i) the surface coverage at the onset of saturation and (ii) any size change. The number of surface atoms per gold particle was calculated using the formula $4\pi R^2(a^2/2)$ divided by $(4/3)\pi R^3(a^3/4)$ where R is the particle radius (5 nm) and a is the lattice parameter (i.e. 0.408 nm for face-centered-cubic gold). For each 5 nm particle (approximately 3800 atoms), approximately 12% (or 470 atoms) are surface atoms. The total number of surface atoms per cuvette was thus 7.5×10^{16} . The number of mercury atoms was calculated from the known concentration of mercury in the nitrogen carrier stream, the carrier stream flowrate (140 ccm), the molecular weight of mercury, Avogadro's number, and the exposure time. For case (c), cuvette #1, the number of mercury atoms per gold surface atom was estimated to be 28 at the onset of saturation, assuming 48% of the mercury atoms were captured in cuvette #1. This is an exceedingly large number of mercury atoms and is most likely an overestimation for several reasons (see below).

After the exposure process, the spectra of the colloidal solutions were observed to relax toward their original position (not shown). The phenomenon behind this relaxation process is not fully understood and is currently under investigation. Two explanations are possible; (i) the mercury atoms slowly diffuse into the interior of the gold particles thereby returning the surface of the particles to their original state, or (ii) the mercury dissolves from the surface of the gold particles. At this time, it is not known to what extent the mercury originally adsorbed onto the surface of the gold particles diffuses into the interior of the grains. In a long-term (greater than 850 days) experiment to determine whether dissolved mercury could be transported through sediment (i.e., quartz sand, granules, and pebbles) and deposited as amalgam on gold grains. Miller *et al.* [26] observed that mercury first deposited on the gold grains subsequently, for some unknown reason, dissolved from the gold. They comment that apparently well aerated conditions, organisms (micro-biota), and bio-physiochemical parameters other than mercury concentration are expected to have a significant effect on the precipitation and dissolution of mercury in the system.

The physical or chemical interaction between the mercury and gold atoms is an important mechanism in the overall process. Extensive work has been done at a macroscopic level and in many cases classical thermodynamics and well defined surface properties are sufficient to describe and/or predict the interaction. For example, the room-temperature surface tension of mercury (485.48 mN/m) is greater than that of water (71.99 mN/m) but less than that of gold (approx. 1.4 mN/m) at 25 °C [1c]). Thus, for bulk gold in water, mercury is expected to adsorb readily onto the gold surface [29, 30]. On a macroscopic level, mercury can combine with gold to form a wide range of intermetallic compounds ranging from AuHg₂ to Au₈Hg [30]. Precisely which intermetallic, or combination of, is formed depends on the nucleation and growth kinetics and is the subject of much debate [31]. From a nano viewpoint, the system is inherently more complicated. First, the phase diagram for bulk Au-Hg cannot be used; by their very nature, phase diagrams only consider systems that are in thermodynamic equilibrium. They give no clues to the rates of reaction, render no information on the effect of point or line defects or the phase distribution morphology, and do not account for surface energy effects at phase boundaries and strain energy effects in transformations [31, 32]. These factors are critically important at the nanoscale and thus the prediction of the interaction between the mercury atoms and gold nanoparticles is a challenging task. Several notable studies have been conducted at the nanoscale (see for example [3, 33-36]), however the majority relate to thin (80–100 nm thick) gold films as opposed to gold nanoparticles. The corrugated, step like surface of nanoparticles and the larger number of grain boundaries is expected to have a significant effect on the amalgamation process.

Fig. 8 shows TEM images of the gold particles before and after exposure to elemental mercury at 1.6 ppm in nitrogen for 60 mins. After exposure, the theoretical maximum number of mercury atoms per gold surface atom was estimated to be 2.4. Allowing for losses (e.g. sorption of mercury atoms to the surface of the tubing, dissolution of mercury into the water, etc.) the number of mercury atoms per gold surface atom is likely to be less. The TEM images revealed no change to the size of the gold particles suggesting that the number of mercury atoms is only a fraction of the number of surface atoms. If 2.4 mercury atoms were adsorbed to the surface of each gold atom, the particle size would be expected to increase by approximately 9% to 5.5 nm. It is interesting to note that before exposure, the gold nanoparticles were randomly dispersed and there was little evidence of any particle aggregation. After exposure however, the particles were clumped together and large aggregates or clusters up to 50-60 nm (see Fig. 9) were formed. From Fig. 2, such clusters would be expected to yield a significant red-shift in the SPR wavelength. However, since no such shift was observed, it is most probable that the particles aggregated whilst the solution dried on the TEM grid. In any case, it can be concluded that the surface properties of the particles are changed after exposure to mercury. It is this change that is most likely responsible for the change in the optical characteristics of the colloidal solution.

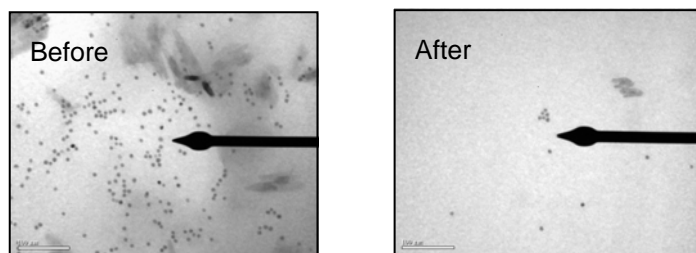


Fig. 8. TEM images of the gold particles before (left) and after (right) exposure to elemental mercury in nitrogen at 1.6 ppm for 60 minutes (i.e., case (b), cuvette #1). After exposure, the number of mercury atoms per gold surface atom was estimated to be 3.4.

5. Conclusions

This study provides a framework for the development of a colorimetric, nano-material based sensor for the detection of elemental mercury. We have exposed surface radiating colloidal gold nanoparticles to mercury at sub-ppm concentrations in air and have demonstrated that the SPR phenomenon can be used as an analytical tool to detect and quantify the amount of mercury sorbed to the surface of the gold particles. The evolution of the SPR wavelength both during and after the exposure process is determined to be a surface-effect, as opposed to a size-effect, and is not well explained by classical electrodynamic theory. The SPR wavelength and absorbance moved linearly with (i) the exposure time and (ii) the increase in electron density, provided the mercury concentration (C_{Hg}) was within a specified range ($\text{DL} < C_{\text{Hg}} < \text{saturation limit}$). The shift in the SPR wavelength was chosen as the most suitable metric to detect and quantify the amount of mercury as its position is independent of particle concentration. That is, the molar absorptivity of the colloidal solution at a particular wavelength is independent of the number of particles in solution, assuming Beer's law is applicable.

In addition to mercury concentration, a further constraint is the instability of the gold particles after exposure to various contaminants. For more complicated systems, e.g. mercury in soil, the colloidal particles aggregated almost immediately and the SPR band disappeared. To overcome this deficiency, we are currently immobilizing different types of gold nanoparticles to transparent, organosilane functionalized quartz (SiO_2) substrates. Preliminary results are promising and set the framework for a reliable, reusable, portable, low-cost mercury detector.

Acknowledgements

This work was funded by the NIEHS Superfund Basic Research Program, and NIH Grant P42-ES047050-01. Use the Acknowledgements section if it is necessary.

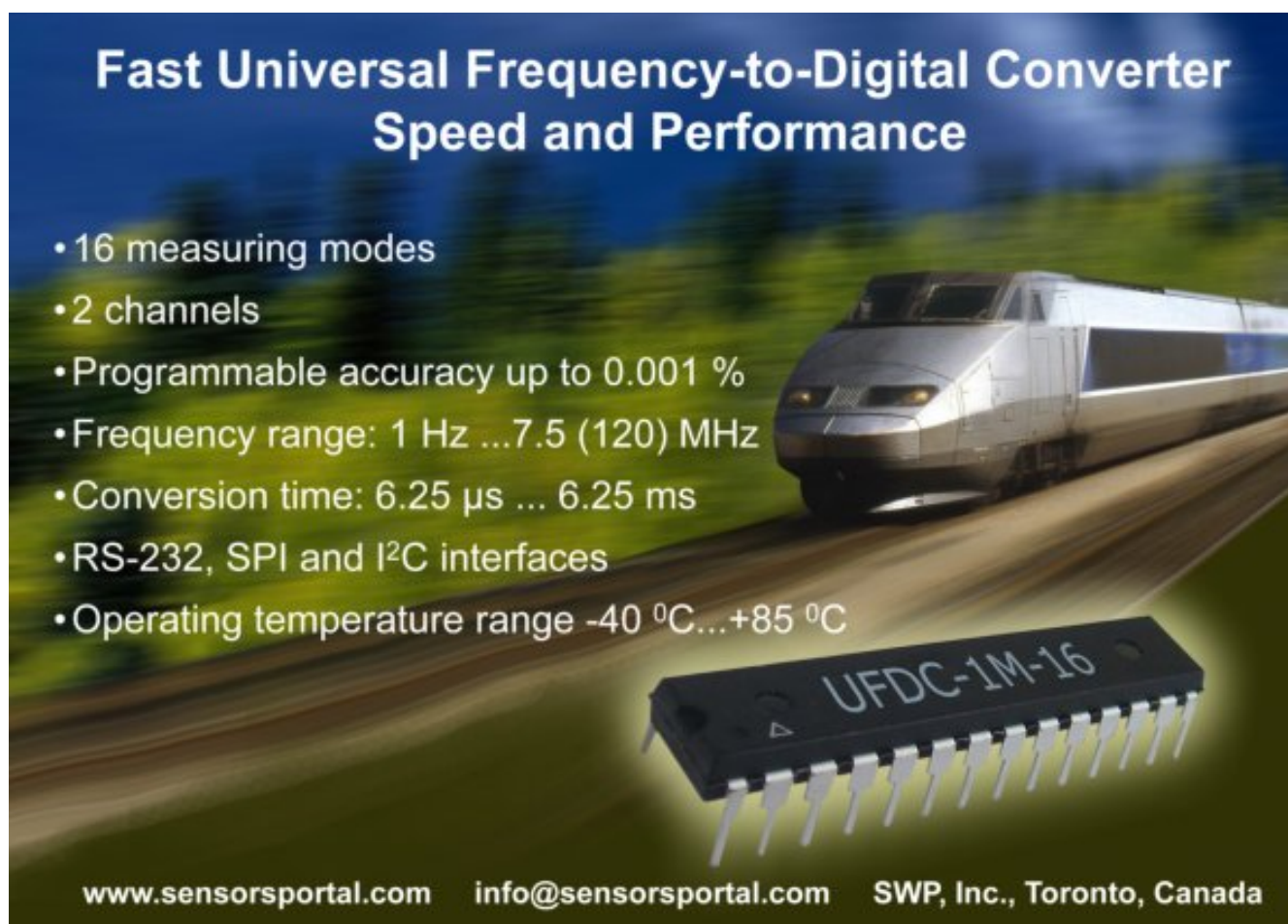
References

- [1]. Handbook of Chemistry & Physics, 79th ed. Lide, D. R., *CRC Press*, 1999 (a) Multiple references, Vapor pressure and IUPAC recommended data for vapor pressure calibration, 6-60–6-87, 6-99; (b) Weaver, J. H., & Frederikse, H. P. R., Optical properties of Metals and Semiconductors, pp. 12-131; (c) Multiple references, Properties of water in the range 0–100 °C, pp. 6-3.
- [2]. M. M. F. Morel, A. M. L. Kraepiel and M. Amyot, The chemical cycle and bioaccumulation of mercury, *Annual Review of Ecology and Systematics*, 29, 1998, pp. 543–566.
- [3]. T. T. Mercer, Adsorption of mercury vapor by gold and silver, *Analytical Chemistry*, 51, 7, 1979, pp. 1026-1030.
- [4]. K. Pleijel and J. Munthe, Modeling the atmospheric mercury cycle – chemistry in fog droplets, *Atmos.*

- Environ.*, 29, 1995, pp. 1441-1457.
- [5]. Siegneur, C., Wrobel, J., and Constantinou, E., A chemical kinetic mechanism for atmospheric inorganic mercury, *Environmental Science Technology*, 28, 1994, pp. 1589-1597.
- [6]. Loux, N. T., Diel temperature effects on the exchange of elemental mercury between the atmosphere and underlying waters, *Environmental Toxicology and Chemistry*, 19, 1999, pp. 1191-1198.
- [7]. Gilmour, C. C. and Henry, E. A., Mercury methylation in aquatic systems affected by acid deposition, *Environmental Pollution*, 71, 2-4, 1991, p. 131.
- [8]. Carpi, A., Mercury from combustion sources: a review of the chemical species emitted and their transport in the environment, *Water, Air, and Soil Pollution*, 98, 1997, pp. 241-254.
- [9]. EPA, 2005, United States Environmental Protection Agency, US EPA, *Clean air mercury rule*, introduced March 15th, 2005. <http://epa.gov/air/mercuryrule/>, November 2006.
- [10]. Kim, Y., Johnson, R. C. and Hupp, J. T., Gold nanoparticle-based sensing of "spectroscopically silent" heavy metal ions, *NanoLetters*, 1, 4, 2001, pp. 165-167.
- [11]. Mirsky, V. M., New electroanalytical applications of self-assembled monolayers, *Trends in Analytical Chemistry*, 21, 6, 7, 2002, p. 439.
- [12]. Liz-Marzan, L. M., Nanomaterials: formation and color, *Materials Today, Elsevier Ltd.*, 2004.
- [13]. Alvarez, M. M., Khoury, J. T., Schaaff, T. G., Shafiqullin, M. N., Vezmar, I., and Whetten, R. L., Optical absorption spectra of nanocrystal gold molecules, *Journal of Physical Chemistry B*, 101, 1997, pp. 3706-3712.
- [14]. Link, S. and El-Sayed, M. A., Size and temperature dependence of the plasmon absorption of colloidal gold nanoparticles, *Journal of Physical Chemistry B*, 103, 1999, pp. 4212-4217.
- [15]. Kreibig, U. and Vollmer, M., Optical Properties of Metal Clusters, *Springer*, Berlin, 1995.
- [16]. Bohren, C. F. and Huffman, D. R., 1983, Adsorption and Scattering of Light by Small Particles, *John Wiley and Sons*, New York.
- [17]. Willner, I., Katz, E., and Shipway, A., Nanoparticle arrays of surfaces for electronic, optical, and sensor applications, *ChemPhysChem.*, 1, 2000, pp. 18-52.
- [18]. Mie, G., Beitrage zur optik truber medien, speziell kolliodaler metallösungen, Leipzig, *Ann. Phys.*, 25, 4, 1908, pp. 377-445.
- [19]. Moriarty, P. Nanostructured materials, *Institute of Physics Publishing, Reports on Progress in Physics*, 64, 2001, pp. 297-381, PII: S0034-4885(01)04041-6.
- [20]. Jain, P. K., Seok Lee, K., El-Sayed, I. H., and El-Sayed, M. A., Calculated absorption and scattering properties of gold nanoparticles of different size, shape, and composition: applications in biological imaging and biomedicine, *Journal of Physical Chemistry B*, 110, 2006, pp. 7238-7248.
- [21]. Muskens, O., Christofilos, D., Del Fatti, N., and Vallee, F., Optical response of a single noble metal nanoparticle, *Journal of Optics A: Pure and Applied Optics.*, 8, 2006, pp. S264-S272.
- [22]. Scaffardi, L. B., Pellegrini, N., de Sanctis, O., and Tocho, J. O., Sizing gold nanoparticles by extinction spectroscopy, *Nanotechnology*, 16, 2005, pp. 158-163.
- [23]. Henglein, A., Physicochemical properties of small metal particles in solution: "microelectrode" reactions, chemisorption, composite metal particles, and atom-to-metal transition, *Journal of Physical Chemistry*, 97, 1993, pp. 5457-5471.
- [24]. Hovel, H., Fritz, S., Hilger, A., and Kreibig, U., Width of cluster plasmon resonances: bulk dielectric functions and chemical interface damping, *Physical Review B*, 48, 24, 1993, p. 18179.
- [25]. Poindexter, Mercury vapor pressure at low temperatures, *Physics Review*, 26, 1925, p. 859.
- [26]. Miller, J. W., Callahan, J. E., and Craig, J. R., Mercury interactions in a simulated gold placer, *Applied Geochemistry*, 17, 2002, pp. 21-28.
- [27]. Morris, T., Novel spectroscopic methods to monitor mercury adsorption to gold and silver surfaces, *Ph. D. Research Seminar, Department of Chemistry, University of Alabama, January 28th*, 2003.
- [28]. Sanemasa, I., The solubility of elemental mercury vapor in water, *Bulletin of the Chemical Society of Japan*, 48, 1975, pp. 1795-1798.
- [29]. Lee, J., Nakamoto, M., and Tanaka, T., Thermodynamic study on the melting of nanometer-sized gold particles on graphite substrate, *Proceeding of the IV International conference/High Temperature Capillarity, Journal of Materials Science*, 40, 2005, pp. 2167-2171.
- [30]. Veiga, M. and Baker, R., Global Mercury Project, Project EG/GLO/01/G34; Removal of barriers to introduction of cleaner artisanal gold mining and extraction technologies: protocols for environmental and health assessment or mercury released by artisanal and small-scale gold miners, UNIDO, Vienna, 2004.
- [31]. Intermetallic Compounds, *Intermetallic Compounds: Principles and Practice*, v. 1, Editors: Westbrook, J. H. and Fleischer, R. L., *Wiley*, New York, 1995.

- [32].Prince, A., Alloy Phase Equilibria, *Elsevier*, New York, 1966.
- [33].Himmelhaus, M., Buck, M., and Grunze, M., Mercury induced reorientation of alkanethiolates adsorbed on gold, *Applied Physics B*, 68, 1999, pp. 595-598.
- [34].Levlin, M. Ikavalko, E., and Laitinen, T., Adsorption of mercury on gold and silver surfaces, *Fresenius Journal of Analytical Chemistry*, 365, 1999, pp. 577-586.
- [35].Nowakowski, R., Kobiela, T., Wolfram, Z., and Dus, R., Atomic force microscopy of Au/Hg alloy formation on thin Au films, *Applied Surface Science*, 115, 1997, pp. 217-231.
- [36].Battistoni, C. Bemporad, E., Galdikas, A., Kaciulis, S., Mattogno, G., Mickevicius, S., and Olevano, V., Interaction of mercury vapor with thin films of gold, *Applied Surface Science*, 103, 1996, pp. 107-111.
-

2007 Copyright ©, International Frequency Sensor Association (IFSA). All rights reserved.
(<http://www.sensorsportal.com>)



Fast Universal Frequency-to-Digital Converter
Speed and Performance

- 16 measuring modes
- 2 channels
- Programmable accuracy up to 0.001 %
- Frequency range: 1 Hz ...7.5 (120) MHz
- Conversion time: 6.25 μ s ... 6.25 ms
- RS-232, SPI and I²C interfaces
- Operating temperature range -40 °C...+85 °C

UFDC-1M-16

www.sensorsportal.com info@sensorsportal.com SWP, Inc., Toronto, Canada

Guide for Contributors

Aims and Scope

Sensors & Transducers Journal (ISSN 1726- 5479) provides an advanced forum for the science and technology of physical, chemical sensors and biosensors. It publishes state-of-the-art reviews, regular research and application specific papers, short notes, letters to Editor and sensors related books reviews as well as academic, practical and commercial information of interest to its readership. Because it is an open access, peer review international journal, papers rapidly published in *Sensors & Transducers Journal* will receive a very high publicity. The journal is published monthly as twelve issues per annual by International Frequency Association (IFSA). In addition, some special sponsored and conference issues published annually.

Topics Covered

Contributions are invited on all aspects of research, development and application of the science and technology of sensors, transducers and sensor instrumentations. Topics include, but are not restricted to:

- Physical, chemical and biosensors;
- Digital, frequency, period, duty-cycle, time interval, PWM, pulse number output sensors and transducers;
- Theory, principles, effects, design, standardization and modeling;
- Smart sensors and systems;
- Sensor instrumentation;
- Virtual instruments;
- Sensors interfaces, buses and networks;
- Signal processing;
- Frequency (period, duty-cycle)-to-digital converters, ADC;
- Technologies and materials;
- Nanosensors;
- Microsystems;
- Applications.

Submission of papers

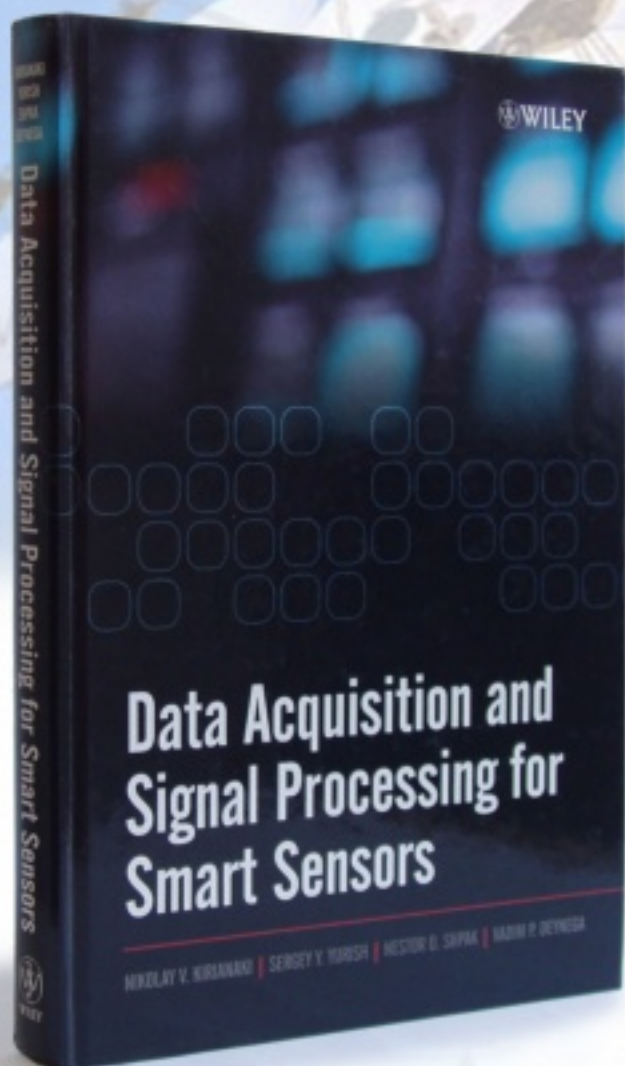
Articles should be written in English. Authors are invited to submit by e-mail editor@sensorsportal.com 6-14 pages article (including abstract, illustrations (color or grayscale), photos and references) in both: MS Word (doc) and Acrobat (pdf) formats. Detailed preparation instructions, paper example and template of manuscript are available from the journal's webpage: <http://www.sensorsportal.com/HTML/DIGEST/Submission.htm> Authors must follow the instructions strictly when submitting their manuscripts.

Advertising Information

Advertising orders and enquires may be sent to sales@sensorsportal.com Please download also our media kit: http://www.sensorsportal.com/DOWNLOADS/Media_Kit_2007.PDF



KNOWLEDGE FOR GENERATIONS



'This book provides a good basis for anyone entering or studying the field of smart sensors not only for the inexperienced but also very useful to those with some experience'

(from IEEE Instrumentation & Measurement Magazine review)



Order online:

http://www.sensorsportal.com/HTML/BOOKSTORE/DAQ_SP.htm

www.sensorsportal.com